

Instruments Designed for Teaching

DRAFT
6/02

OPTICAL PUMPING OF RUBIDIUM

Guide to the Experiment

INSTRUCTOR'S MANUAL

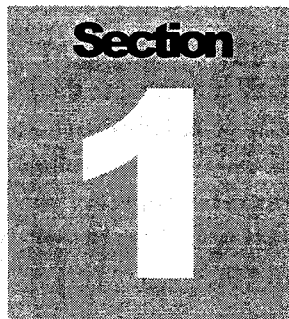
A PRODUCT OF TEACHSPIN, INC.

TeachSpin, Inc. 45 Penhurst Park, Buffalo, NY 14222-1013
(716) 885-4701 or www.teachspin.com

Copyright © June 2002

Table of Contents

| SECTION | PAGE |
|---|------|
| 1. Introduction | 1-1 |
| 2. Theory | |
| A. Structure of alkali atoms | 2-1 |
| B. Interaction of an alkali atom with a magnetic field | 2-2 |
| C. Photon absorption in an alkali atom | 2-8 |
| D. Optical pumping in rubidium | 2-11 |
| E. Zero field transition | 2-14 |
| F. Rf spectroscopy of Rb ⁸⁵ and Rb ⁸⁷ | 2-15 |
| G. Transient effects | 2-17 |
| 3. Apparatus | |
| A. Rubidium discharge lamp | 3-1 |
| B. Detector | 3-3 |
| C. Optics | 3-5 |
| D. Temperature regulation | 3-10 |
| E. Magnetic fields | 3-14 |
| F. Radio frequency | 3-19 |
| 4. Experiments | |
| A. Absorption of Rb resonance radiation by atomic Rb | 4-1 |
| B. Low field resonances | 4-6 |
| C. Quadratic Zeeman Effect | 4-12 |
| D. Transient effects | 4-17 |
| 5. Getting Started | 5-1 |



INTRODUCTION

The term "optical pumping" refers to a process which uses photons to redistribute the states occupied by a collection of atoms. For example, an isolated collection of atoms in the form of a gas will occupy their available energy states, at a given temperature, in a way predicted by standard statistical mechanics. This is referred to as the thermal equilibrium distribution. But the distribution of the atoms among these energy states can be radically altered by the clever application of what is called "resonance radiation."

Alfred Kastler, a French physicist, introduced modern optical pumping in 1950 and, in 1966, was awarded a Nobel Prize "*for the discovery and development of optical methods for studying hertzian resonances in atoms.*" In these laboratory experiments you will explore the phenomenon of optical pumping and its application to fundamental measurements in atomic physics. It is not likely that you will have time to study all the possible experiments that this instrument is capable of performing, but you should have ample opportunity to explore many interesting phenomena. The apparatus has deceptively simple components, yet it is capable of exploring very complex physics.

The atom you will be exploring is rubidium. It is chosen because of its hydrogen-like qualities. That is, it is a very good approximation to consider this atom as a one-electron atom, since the "core" electrons form a closed shell, noble gas configuration. The rubidium atoms are contained within a sealed glass bulb along with 30 torr of the noble gas neon. Ideally, if one were studying the metrology of the energy state of rubidium, one would want to have the atoms in vacuum at extremely low density, so they would not interact. Such systems do exist; they are called an atomic beam apparatus, but they are very large and expensive instruments which have their own serious limitations. The addition of neon, as a "buffer gas," in a small contained volume, greatly simplifies the apparatus and the experiments. Because of the spherical symmetry of the electronic ground state of neon, collisions between a rubidium and neon atom do not exchange angular momentum. This turns out to be crucial for performing optical pumping experiments.

You will probably need to review your atomic physics and possibly your optics. The use of circularly polarized light is also crucial to the optical pumping process. We strongly urge you to review these subjects as well as to look up most of the references given in this manual. Although the basic process was discovered over 50 years ago, the topic is very current.

Optical pumping is the basis of all lasers; it is an important tool for studying collision and exchange relaxation processes, and also finds applicability in both solid state and liquid state physics. A good article to start your reading might be Thomas Carver's review article in Science 16 August, 1963 Vol. 141, No. 3581. There is also a set of reprints called MASERS AND OPTICAL PUMPING, AAPT Committee Resource Letters, published in 1965. Look them up.

Have fun!

THEORY

2A. Structure of Alkali Atoms

In these experiments, we will study the absorption of light by rubidium atoms, and, as a prelude to that, we will consider the atomic structure of the rubidium atom. In the quantum mechanical model we will consider, atoms are described in terms of the central field approximation in which the nucleus is taken to be a point particle characterized by its only observable properties of charge, spin angular momentum, and electric and magnetic moments. The energy levels can be described by angular momentum wave functions that can be calculated generally from the angular parts of the separated Schrodinger equation. These functions are applied in a perturbation theory approach to calculate the eigenstates of the atom. In the case of the alkali atoms, the angular momenta are coupled in what is called the Russell-Saunders coupling scheme, which yields energy level values close to those observed.

All of the alkali atoms are similar in structure to the hydrogen atom. That is, many of their properties are determined by a *single* valence electron. Rubidium, which has an atomic number of 37, can be described by means of an electronic configuration (in the standard notation):

$$1s^2 2s^2 2p^6 3s^2 3p^6 3d^{10} 4s^2 4p^6 5s^1$$

where the superscripts are the number of electrons in each shell [2A-1]. The electrons in the inner shells are paired, and to the approximation necessary here, we can completely neglect the presence of the inner electrons, and concentrate our attention on the single outer electron. That is, the entire discussion of all our optical pumping experiments will be based on a model that considers a free rubidium atom as if it was a simple hydrogenic single electron atom.

The outer electron can be described by means of an orbital angular momentum L , a spin angular momentum S , and a total non-nuclear angular momentum J , all in units of \hbar . Since these are all vectors they can be combined by the usual rules as shown in Figure 2A-1. Each of these angular momenta has a magnetic dipole moment associated with it, and they are coupled by a magnetic interaction of the form $\mu_L \cdot \mu_S$. As is the case with classical angular momenta, different orientations of the vectors lead to different interaction energies. Here, however, the values of energy that result are quantized, and can have only allowed values.

As can be seen from the figure, the total angular momentum can be written as

$$\mathbf{J} = \mathbf{L} + \mathbf{S}$$

In the absence of any further interactions \mathbf{J} will be a constant of the motion.

In the electronic ground state of an alkali atom the value of \mathbf{L} is zero, as it is in the hydrogen atom. Since a single electron has an intrinsic spin angular momentum of $\hbar/2$, the value of \mathbf{S} will be $1/2$, and the total angular momentum will have a value of $S = 1/2$.



FIGURE 2A-1. Angular momentum coupling in the valence electron of an alkali atom.

In spectroscopic notation, the electronic state is written $^{2S+1}L_J$, so the ground state of an alkali atom is designated $^2S_{1/2}$. The first excited state has an L value of $1 \ h$, and is designated as a P state. Higher values of L are given the label D, F, ... by convention.

In the case of the P state, J can only have the values $L + S$ and $L - S$. Thus, there are only two P states, $^2P_{1/2}$ and $^2P_{3/2}$, for the single electron in an alkali atom. These states have different energies. This energy splitting, called the **Fine Structure**, is shown diagrammatically in Figure 2A-2. Please note, Figure 2A-2 is not to scale! The fine structure splitting is **much, much, much**, smaller than the energy difference between the ground state and the first excited state.

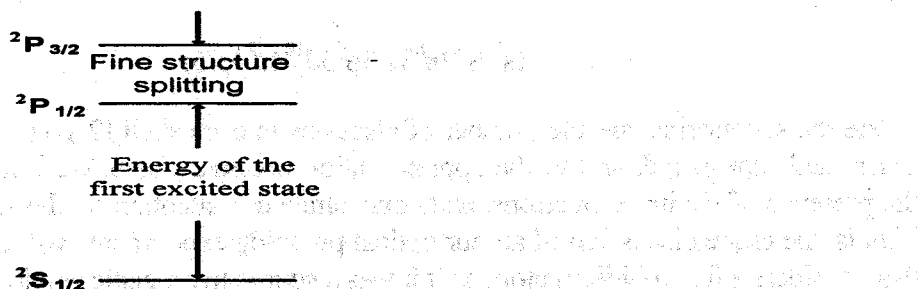


FIGURE 2A-2. Energy level diagram of an alkali atom.
We must now take into account the properties of the nucleus of the atom. In particular we must consider the nuclear spin and the nuclear magnetic dipole moment. Many nuclei have an intrinsic angular momentum, similar to that of the electron, with different values depending on the nucleus.

Associated with this spin is a magnetic dipole moment. In the approximation that we are considering here, the nuclear moment will couple with the electronic magnetic dipole moment associated with \mathbf{J} to form a total angular momentum of the atom, \mathbf{F} . In the context of the vector model the coupling is as shown in Figure 2A-3.

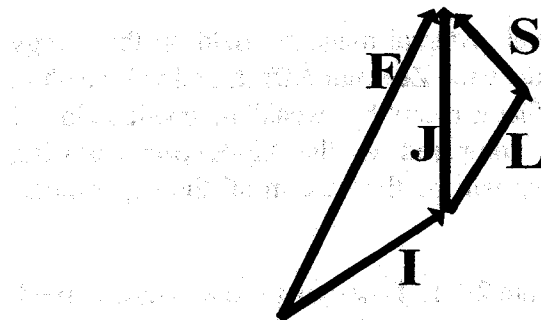


FIGURE 2A-3. Hyperfine coupling in an alkali atom.

The nuclear spin is denoted by \mathbf{I} , the interaction is again of the form $\mu_I \cdot \mu_J$, and the result is a further splitting of the energy levels called the **Hyperfine Structure**. This energy can be characterized by a Hamiltonian as

$$\mathcal{H} = ha \mathbf{I} \cdot \mathbf{J} \quad 2A-1$$

where h is Planck's constant and a is a constant that is different for each electronic state and is determined experimentally. The eigenvalues of this Hamiltonian give the interaction energies as shown in Figure 2A-4.

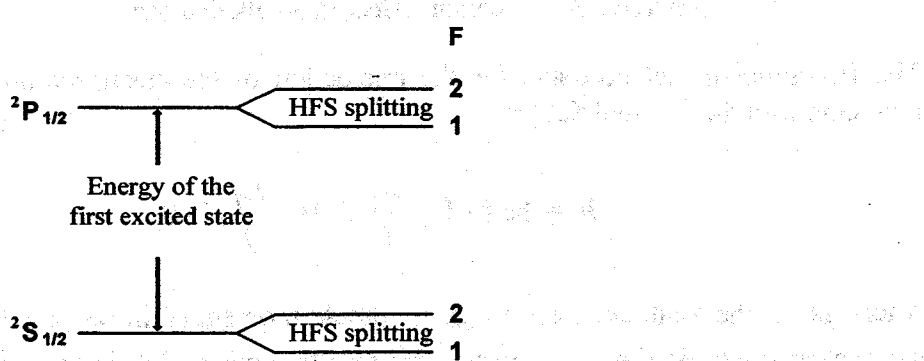


FIGURE 2A-4. Hyperfine splitting for $I = 3/2$

REFERENCES

- [2A-1] J. C. Slater, "Quantum Theory of Atomic Structure" (McGraw-Hill, New York, 1960).

2B. Interaction of an Alkali Atom with a Magnetic Field

We must now consider the effect of a weak external magnetic field on the energy levels of our alkali atom. This will produce the **Zeeman Effect**, and will result in further splitting of the energy levels. What is meant by "weak" magnetic field? If the resulting splitting is very small compared to the **Hyperfine Splitting** (HFS), the magnetic field is said to be weak. This will be the case in all the experiments discussed here.

A vector diagram for an alkali atom is shown in Figure 2B-1. \mathbf{B} designates the magnetic field, and \mathbf{M} is the component of \mathbf{F} in the direction of the magnetic field. \mathbf{F} precesses about the magnetic field at the **Larmour frequency**.

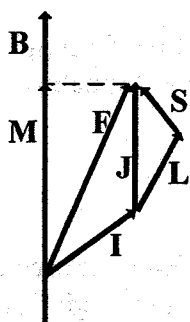


FIGURE 2B-1. Zeeman effect in an alkali atom.

The Hamiltonian that accounts for the interaction of the electronic and nuclear magnetic moments with the external field is

$$\mathcal{H} = \hbar \omega (\mathbf{I} \cdot \mathbf{J} - \frac{\mu_J}{J} \mathbf{J} \cdot \mathbf{B} - \frac{\mu_I}{I} \mathbf{I} \cdot \mathbf{B}) \quad 2B-1$$

where μ_J is the total electronic magnetic dipole moment (spin coupled to orbit), and μ_I is the nuclear magnetic dipole moment. The resulting energy levels are shown in Figure 2B-2 for the $^2S_{1/2}$ ground electronic state with a positive nuclear magnetic moment and a nuclear spin of $3/2$. The levels are similar for the $^2P_{1/2}$ state. For reasons that will become clear later, we will ignore the $^2P_{3/2}$ state. As can be seen from Figure 2B-2 the magnetic field splits each F level into $2F + 1$ sublevels that are approximately equally spaced. In actuality, they vary in their spacing by a small amount determined by the direct interaction of the nuclear magnetic moment with the applied field. We will take advantage of this later on to allow all of the possible transitions to be observed.

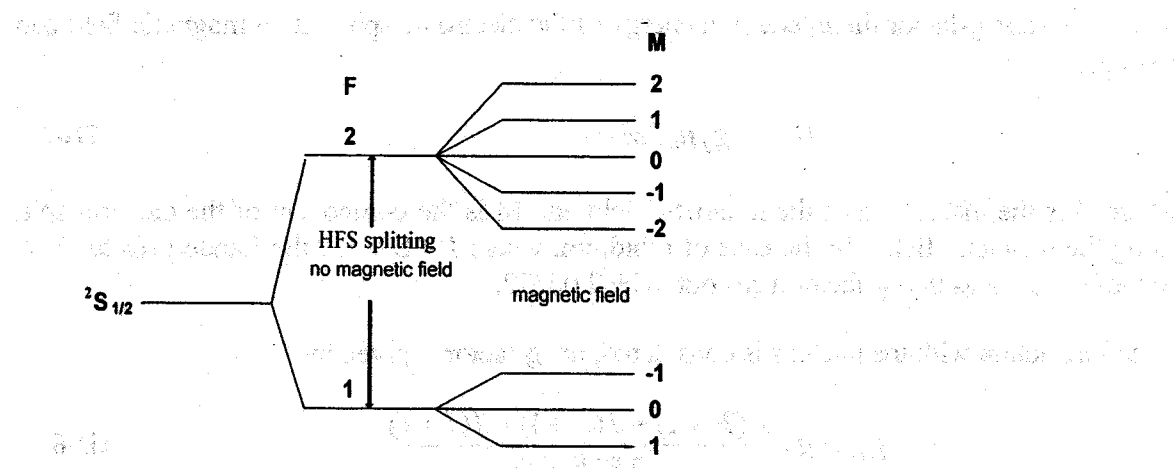


FIGURE 2B-2. Energy levels of an alkali atom in the $^2S_{1/2}$ state with a nuclear spin of $3/2$ and a positive nuclear magnetic dipole moment in a weak magnetic field.

In the case of an atom with either $J = 1/2$ or $I = 1/2$ the energy levels can be calculated in closed form from quantum mechanics. This solution is called the Breit-Rabi equation. To proceed further, we need to consider the atom-magnetic field interaction in more detail. A single electron has spin of $1/2$ and an electrical charge of about 1.6×10^{-19} coulomb. In the simplest picture, this rotating charge gives rise to a magnetic dipole moment whose magnitude is equal to μ_0 , the Bohr magneton. If the electron is bound in an atom, its effective magnetic moment changes and is best described by means of the Lande g-factor.

If the nucleus is neglected, the vector model [2B-1] is used to write the energy of interaction of an atom with an external magnetic field as

$$\text{Magnetic energy} = \frac{M[(L + 2S)\bar{J}]}{J^2} \mu_0 B = g_J \mu_0 M B \quad 2B-2$$

where g_J , known as the **Lande g-factor**, is given by

$$g_J = \frac{(L + 2S)\bar{J}}{J^2} \quad 2B-3$$

This can be evaluated from the vector model to be

$$g_J = 1 + \frac{J(J+1) + S(S+1) - L(L+1)}{2J(J+1)} \quad 2B-4$$

In terms of this g-factor the interaction energy of the electronic spin with a magnetic field can be expressed as

$$W = -g_J \mu_0 B M \quad 2B-5$$

where B is the magnitude of the magnetic field and M is the component of the electron spin along the magnetic field. In the case of rubidium, where $J = S = 1/2$ the Lande g-factor is 2. Actually, the measured g-factor turns out to be 2.00232.

If the interaction with the nucleus is considered, the g-factor is given by

$$g_F = g_J \frac{F(F+1) + J(J+1) - I(I+1)}{2F(F+1)} \quad 2B-6$$

The interaction energy is then given by

$$W = g_F \mu_0 B M \quad 2B-7$$

where the direct interaction of the nuclear moment with the magnetic field is being neglected.

The above results are satisfactory as long as the interaction energy with the magnetic field is small, and the energy levels depend only linearly on the magnetic field. For the purposes of our experiment, we need to consider terms quadratic in the field. Equation 2B-1 can be diagonalized by standard methods of perturbation theory. The result is the Breit-Rabi equation

$$W(F, M) = -\frac{\Delta W}{2(2I+1)} - \frac{\mu_I}{I} BM \pm \frac{\Delta W}{2} \left[1 + \frac{4M}{2I+1} x + x^2 \right]^{1/2} \quad 2B-8$$

where

$$x = (g_J - g_I) \frac{\mu_0 B}{\Delta W} \quad g_I = -\frac{\mu_I}{I \mu_0} \quad 2B-9$$

W is the interaction energy and ΔW is the hyperfine energy splitting [2B-2].

A plot of the Breit-Rabi equation is shown in Figure 2B-3. The energy is shown on the vertical axis field as the dimensionless number $W/\Delta W$, and the horizontal axis shows the magnetic field as the dimensionless number x. The diagram can be divided into three main parts. The first is the Zeeman region very close to $x = 0$ where the energy level splitting varies linearly with the applied magnetic field. The second is the Paschen-Back region $x > 2$, where the energy levels are again linear in the magnetic field. This corresponds to the decoupling of I and J. The upper group of four levels corresponds to m_J , the projection of J along the axis of the applied magnetic field, having a value of $1/2$, while the four lower levels correspond to $m_J = -1/2$. The individual levels correspond to different values of m_I , the projection of I along the axis of the applied magnetic field.

The third region is the intermediate field region that extends from the Zeeman to the Paschen-Back region. Here, the energy levels are not linear in the applied magnetic field; I and J are decoupling, and M is no longer a "good" quantum number. In the Zeeman region, M is a good quantum number. At high fields m_I and m_J are good quantum numbers and can be used to label the levels. At all fields, $M = m_I + m_J$.

In the optical pumping experiment, we will be concerned with small magnetic fields, where the levels are either linear in the magnetic field, or where there is a small quadratic dependence.

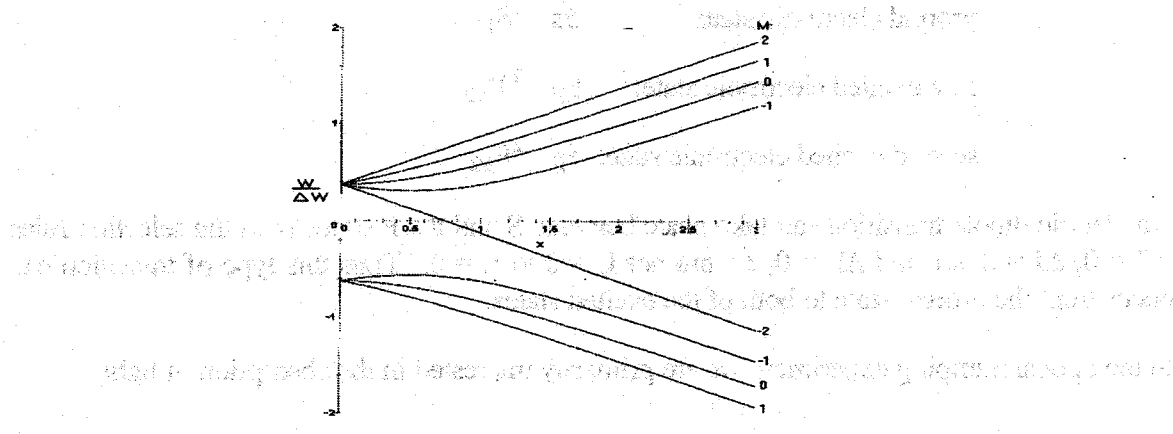


FIGURE 2B-3. Breit-Rabi diagram of an alkali atom in a magnetic field. The nuclear spin is $3/2$ and the nuclear magnetic moment is positive.

REFERENCES

- [2B-1] J. C. Slater, "Quantum Theory of Atomic Structure" (McGraw-Hill, New York, 1960).
- [2B-2] N. F. Ramsey, "Molecular Beams" (Oxford University Press, London, 1969).

2C. Photon Absorption in an Alkali Atom

The three lowest electronic states of an alkali atom are shown in Figure 2A-2. As discussed there, if all filled electron shells are omitted, these three states can be labeled as

ground electronic state: $5s\ ^2S_{1/2}$

first excited electronic state: $5p\ ^2P_{1/2}$

second excited electronic state: $5p\ ^2P_{3/2}$

An electric dipole transition can take place between S and the P states with the selection rules $\Delta S = 0$, $\Delta J = 0, \pm 1$ and $\Delta L = 0, \pm 1$ but not $L = 0$ to $L = 0$. Thus this type of transition can occur from the ground state to both of the excited states.

In the optical pumping experiment we are primarily interested in the absorption of light

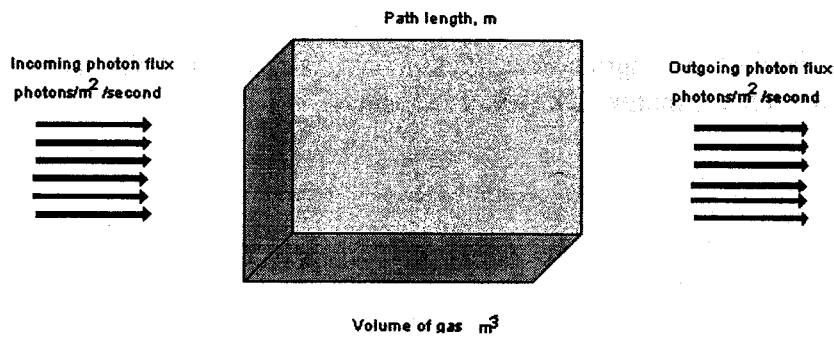


FIGURE 2C-1. Light absorption by a volume of gas.

by a volume of a gas as illustrated in Figure 2C-1. Assuming that the light is resonant with one of the allowed transitions, a fraction of the incident light will be absorbed by the atoms of the gas. Once the atoms have been excited they will decay back to the ground state by spontaneous emission, but since this emission occurs equally in all directions, only a small amount will be radiated into the outgoing beam. For our discussion, this fraction will be ignored.

It is convenient to describe this process using the concept of a "cross section". Suppose for instance, that the incoming beam consisted of electrons instead of photons. In that case, the attenuation of the incoming electrons by the gas atoms can, in the limit of low density, be

described by the simple relation

$$n = n_0 e^{-\sigma \rho l} \quad 2C-1$$

where n_0 and n are the incident and outgoing flux of electrons, ρ is the gas density, l is the path length through the gas, and σ is the cross section. In the case of electron-atom or atom-atom scattering the magnitude of the cross section is of the order of 10^{-20} m^2 , which is $(10^{-10})^2$, and 10^{-10} m is taken to represent the geometrical diameter of the atom.

A similar concept can be applied to the absorption of photons by a volume of gas. Here we write

$$I = I_0 e^{-\sigma_0 \rho l} \quad 2C-2$$

where I_0 and I represent the incident and outgoing flux of photons. If the incident photons are resonant with an atomic transition the observed cross-section will be dramatically different from the geometrical cross-section. In fact, this cross-section is often taken to be of the order of the wavelength of the radiation squared. In this experiment you will attempt to measure the photon absorption cross-section for rubidium resonance radiation on rubidium atoms, and you can compare your measured value with expectations.

The quantity σ_0 is the maximum absorption cross-section measured at the center of the atomic resonance, and it is related to the usual definition of the absorption coefficient by

$$k_0 \equiv \sigma_0 \rho \quad 2C-3$$

For an absorption line that is being broadened only by the Doppler effect, the maximum absorption coefficient can be calculated from

$$k_0 = \frac{2}{\Delta \nu_D} \cdot \frac{\lambda_0^2 g_2}{8\pi g_1} \cdot \frac{\rho}{\tau} \quad 2C-4$$

where λ_0 is the wavelength at the center of the absorption line, $\Delta \nu_D$ is the Doppler width of the absorption line, g_1 and g_2 are the statistical weights of the lower and upper state respectively, and τ is the radiative lifetime of the upper electronic state. The Doppler width can be calculated from

$$\Delta \nu_D = 3 \times 10^{-20} \nu_0 \left(\frac{T}{M} \right)^{\frac{1}{2}} \quad 2C-5$$

where ν_0 is the transition frequency, T is the absolute temperature of the absorbing gas, and M is the mass of the absorbing atom [2C-1].

For optical pumping, we must take the hyperfine structure into account. The energy levels are as shown in Figure 2A-4. Now an additional selection rule, $\Delta F = 0, \pm 1$, must be added for changes in the total angular momentum quantum number. Additional splitting is introduced by an external magnetic field as shown in Figure 2B-2, requiring yet another selection rule $\Delta M = 0, \pm 1$. Thus, the selection rules for an electric dipole transition can be summarized by

Electric dipole transition: $\Delta S = 0, \Delta J = 0, \pm 1, \Delta L = 0, \pm 1$ but not $L = 0$ to $L = 0$
 $\Delta F = 0, \pm 1$ and $\Delta M = 0, \pm 1$

In the emission spectrum of an alkali atom, all transitions obeying the above selection rules are observed, and these give rise to the well-known bright line spectrum (the emission Zeeman effect will be ignored in this discussion). In absorption, however, things can be somewhat different in regard to the selection rule for M . Since angular momentum must always be conserved, the absorption of light in the presence of an applied magnetic field will depend on the polarization of the light and the direction of the incoming beam of light with respect to the direction of the magnetic field. For our purposes we are only interested in the absorption of circularly polarized light that is resonant with the transition from the $^2S_{1/2}$ state to the P states.

In the optical pumping experiment, the direction of the incident light is parallel to the applied magnetic field, and the light is polarized so that it is either right or left circularly polarized. In this arrangement, only transitions in which M changes by $+1$ or -1 are allowed, but not both. Pumping will occur in either case as will be discussed later.

The above discussion applies to allowed electric dipole transitions in an atom. We must also consider magnetic dipole transitions that are about 10^5 times weaker than in the electric dipole case. The transitions in which we will be interested occur in the hyperfine structure and between the magnetic sublevels, and will only be observed in absorption. The selection rules are $\Delta F = 0, \pm 1$ and $\Delta M = 0, \pm 1$. Which transitions occur depends on the orientation of the RF magnetic field with respect to the dc magnetic field.

In our experiment, the RF magnetic field is perpendicular to the dc magnetic field. In this case, the only transitions that can occur have $\Delta F = 0, \pm 1$ and $\Delta M = \pm 1$. The $\Delta F = \pm 1$ transitions occur at RF frequencies of several gigahertz (GHz), and can not be observed with this apparatus. Therefore, we will only be concerned with $\Delta F = 0$ and $\Delta M = \pm 1$.

In the case of allowed electric dipole transitions in emission, the lifetimes of the excited states are of the order of 10^{-8} second resulting in a natural line width of several hundred megahertz (MHz). The actual line width, determined by Doppler broadening, is of the order of one GHz. For magnetic dipole transitions in the hyperfine structure of the ground electronic state, the lifetimes for radiation are much longer, and collision processes will determine the actual lifetimes.

REFERENCES

- [2C-1] Allan C. G. Mitchell and Mark W. Zemansky, "Resonance Radiation and Excited Atoms (Cambridge Univ. Press, 1961).

2D. Optical Pumping in Rubidium

Optical pumping is a method of driving an ensemble of atoms away from thermodynamic equilibrium by means of the resonant absorption of light [2D-1, 2D-2, 2D-3, 2D-4]. Rubidium resonance radiation is passed through a heated absorption cell containing rubidium metal and a buffer gas. The buffer gas is usually a noble gas such as helium or neon. If it were not present, the rubidium atoms would quickly collide with the walls of the cell which would tend to destroy the optical pumping. Collisions with the buffer gas are much less likely to destroy the pumping, thus allowing a greater degree of pumping to be obtained.

The general arrangement of the apparatus is shown in Figure 2D-1.

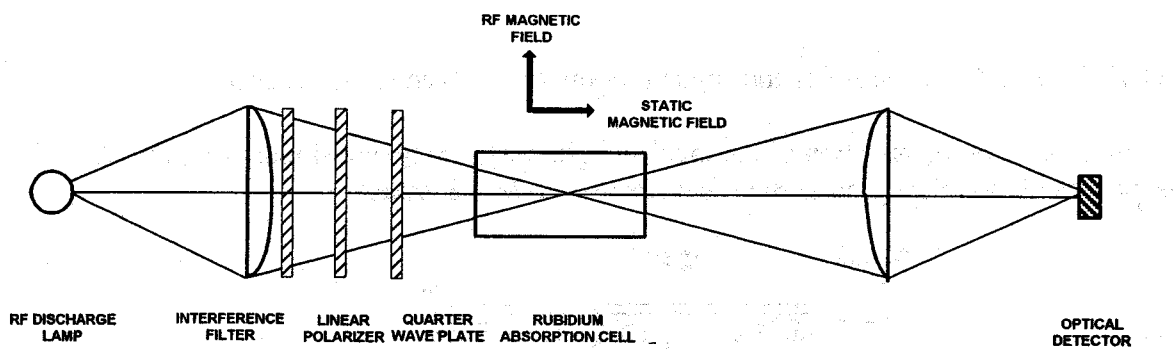


FIGURE 2D-1. Apparatus arrangement for optical pumping.

Resonance light is produced by an RF discharge lamp containing xenon gas and a small amount of rubidium metal, which has been enriched in Rb^{87} such that there are equal amounts of natural Rb and Rb^{87} . The gas is excited by an oscillator operating at a frequency of about 100 MHz. The high electric field produced in the lamp causes ionization in the gas, and the resulting electrons are accelerated sufficiently to excite the rubidium atoms by collisions. Spontaneous radiation from the excited states produces the emission spectrum of rubidium.

Resonance light from the lamp consists of two main lines one at 780 and one at 795 nm. The 780 nm line is removed by the interference filter and the remaining light is circularly polarized before being passed through the absorption cell. An optical detector monitors the intensity of the transmitted light. A dc magnetic field is applied to the absorption cell along the optical axis, and transitions are induced in the sample by means of a transverse RF magnetic field.

Figure 2D-2 shows the magnetic fields and angular momenta involved in the optical pumping of rubidium. The projection of \mathbf{F} along the magnetic field is the magnetic quantum number M , and this vector precesses about the applied magnetic field at the Larmor frequency. Note that the RF magnetic field is perpendicular to the applied dc magnetic field.

Transitions are induced between electronic energy levels by the optical radiation and between the Zeeman levels by means of the RF magnetic field. The optical transitions are shown schematically in Figure 2D-3 for those energy levels involved in the optical pumping of Rb^{87} which has a nuclear spin of $3/2$. The transitions are shown for the case of $\Delta M = +1$, but the

situation would be similar for $\Delta M = -1$ except that the pumping would go to the $M = -2$ level of $^2S_{1/2}$ electronic ground state.

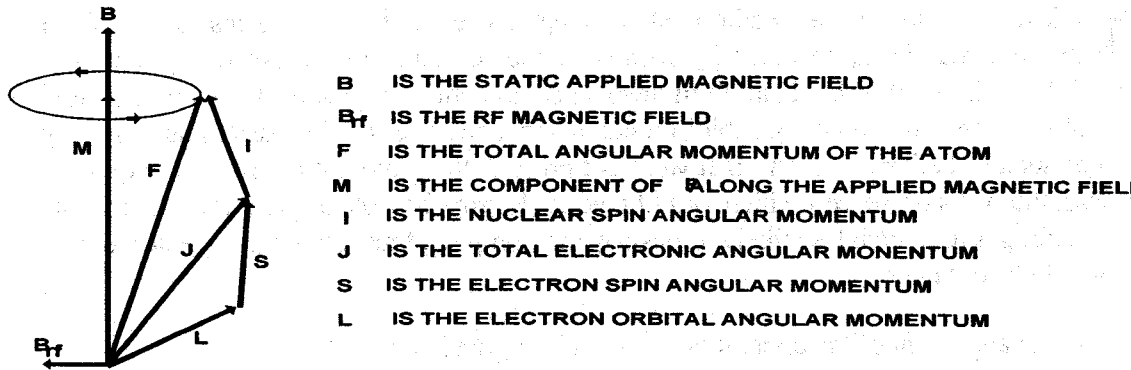


FIGURE 2D-2. Magnetic fields and angular momenta involved in the experiment.

Due to the circular polarization of the incident light, there are no transitions from the $M = +2$ magnetic sublevel of the ground state since there is no $M = 3$ state.

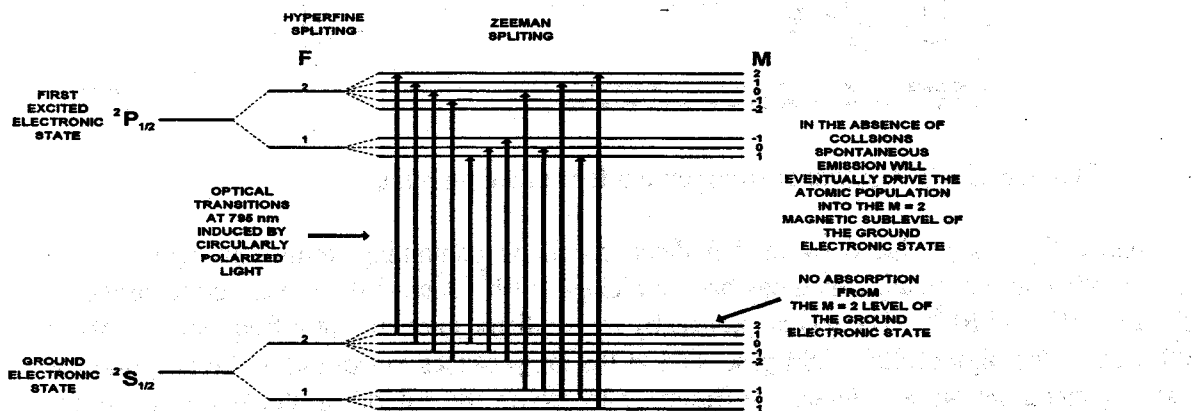


FIGURE 2D-3. Transitions involved in the optical pumping of Rb^{87} .

The excited states can decay back into this level by spontaneous emission or collisions providing a path into the level but not out of it. Hence, the population of this level will increase with respect to the other sublevels. The population of the $M = +2$ level is monitored by the intensity of the transmitted light. Any process that changes this population, such as transitions between the M levels, will change the intensity of this transmitted light.

The intensity of the transmitted light is monitored by a photodiode whose output is amplified and observed on an oscilloscope or other recording device. The RF is set to a predetermined frequency and amplitude, and the magnetic field is slowly varied. The resulting output represents the transmitted light intensity as a function of applied magnetic field.

The optical pumping process itself will be studied in this experiment, and it will be determined that pumping requires a time of 10 – 20 milliseconds to achieve a suitable population of the

$M = +2$ sublevel. Hence, the rate of variation of the magnetic field must be kept small in order for there to be sufficient absorption of the transmitted light.

If the above discussed processes were the only ones that occurred, the result would be a very large increase in the population of the $M = +2$ or $M = -2$ states. However, we must consider collisional processes between the pumped rubidium atoms and other rubidium atoms, and also collisions with atoms of the buffer gas. These collisions can result in transitions between the magnetic substates, and such transitions will tend to equalize the populations and destroy the optical pumping. In actuality, the amount of pumping will be determined by a balance between the rate of transitions into the pumped state, and the rate at which atoms are removed from this state by collisional relaxation processes.

A set of rate equations can be used to describe the pumping process [2D-5]. Consider the isotope Rb ⁸⁷ that has a nuclear spin of 3/2 and a total of 8 magnetic sublevels in the ground electronic state. Let b_{ij} be the probability per unit time that an atom in the sublevel i of the ground state has undergone a transition to the sublevel j of the ground state by absorption and re-emission of a photon. Similarly let w_{ij} be the probability per unit time for the corresponding transition produced by relaxation processes. The occupation probability $p_k(t)$ of the k -th level is obtained by the solution of the following set of eight simultaneous differential equations:

$$\dot{p}_k = - \sum_{j=1}^8 (b_{kj} + w_{kj}) p_k + \sum_{j=1}^8 (b_{ik} + w_{ik}) p_i \quad k = 1, 2, \dots, 8 \quad 2D-1$$

Only seven of these equations are independent since $\sum_k p_k = 1$. The dot denotes

differentiation with respect to time, and the sums should exclude terms in which $j = k$ and $i = k$. For a full discussion see the article by Franzen and Emslie [2D-5]. It is shown there that the population of the $M = +2$ or the $M = -2$ state will increase exponentially with time after the pumping light is turned on and the population of the other M levels will decrease. Thus, an excess population in the level of maximum M will develop, as compared to the population distribution in thermodynamic equilibrium. This is what is meant by the term "optical pumping".

REFERENCES

- [2D-1] Robert L. de Zafra, Am. J. Phys. volume?, 646 (1960).
- [2D-2] William Happer, Rev. Mod. Phys., 44, 169 (1972).
- [2D-3] G. W. Series, Rept. Progr. Phys. 22, 280 (1959).
- [2D-4] Alan Corney, "Atomic and Laser Spectroscopy" (Oxford Univ. Press, 1986).
- [2D-5] W. Franzen and A. G. Emslie, Phys. Rev. 108, 1453 (1957).

2E. Zero Field Transition

Before we consider RF resonances in rubidium it is necessary to discuss the transitions that can be observed at zero magnetic field. Assume that the apparatus is set up as in Figure 2D-1 and that no RF is applied. The magnetic field is now slowly swept around zero, and the intensity of the transmitted light is monitored. A decrease in intensity will be observed as the field goes through zero as shown in Figure 2E-1.

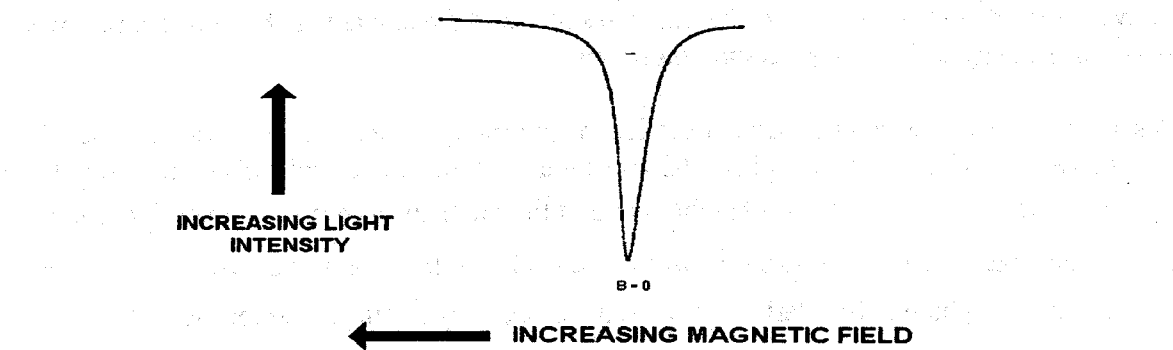


FIGURE 2E-1. Transition at zero magnetic field with no RF.

If the magnetic field is set to zero manually, a dc signal will be observed as a decrease in the intensity of the transmitted light. This can be understood qualitatively by referring to Figure 2E-2 which shows the energy levels near zero magnetic field. To either side of zero field the levels are split in energy, and normal optical pumping occurs. However, at or near zero field, the levels become degenerate; optical pumping does not produce a population imbalance; and more light is absorbed.

The zero field signal provides a good way to determine the parameters for zero total magnetic field within the volume of the absorption cell. If the magnetic field is swept in time, and the output of the optical detector displayed on a scope, the field in the cell can be made as near zero as possible by adjusting the compensating coils and the orientation of the apparatus to achieve minimum line width. The above is true as long as the magnetic field is not swept too rapidly. Fast sweeping will produce time dependent effects which will be discussed later.

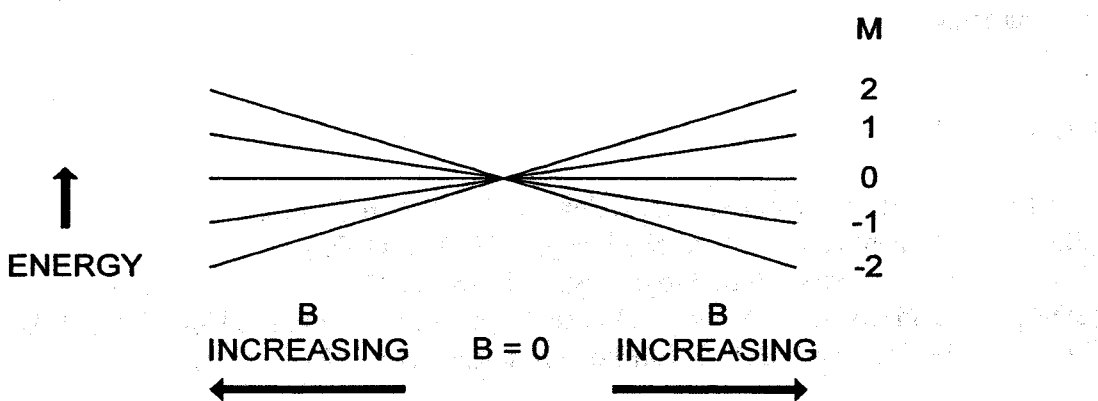


FIGURE 2E-2. Energy levels near zero magnetic field with no RF.

2F. RF Spectroscopy of Rb⁸⁵ and Rb⁸⁷

As mentioned in the previous section, optical pumping drives an atomic system away from thermodynamic equilibrium. Consider the energy levels of the ground electronic state as depicted in Figure 2D-3 which applies to Rb⁸⁷ (nuclear spin of 3/2). We are interested in the levels for atoms in a weak magnetic field (far right of diagram). Since I = 3/2 and J = 1/2, the total angular momentum quantum number has the values of F = 2 or F = 1. The levels would be similar for Rb⁸⁵ except in that case F = 3 or 2.

In thermodynamic equilibrium, the population of the magnetic sublevels of the ground electronic state would be essentially equal, and optical pumping will lead to an excess of population in either the M = 2 or the M = -2 levels. After the pumping light has been on for a sufficient time, of the order of milliseconds, a new equilibrium will be established, and the intensity of the light transmitted by the cell will reflect this new equilibrium. If an RF magnetic field is applied as shown in Figure 2D-1 transitions with $\Delta M = \pm 1$ will be induced, and these will tend to drive the system back toward thermodynamic equilibrium. The result will be a decrease in the intensity of the transmitted light.

Equation 2B-5 gives the relative energy levels of the ground electronic state. We can calculate the resonance transition frequency as

$$W(M+1) - W(M) = g_F \mu_0 B(M+1) - W(M) = g_F \mu_0 B \quad 2F-1$$

$$\nu = g_F \mu_0 B / h \quad 2F-2$$

where ν is the transition frequency in sec⁻¹ and h is Planck's constant. For our experiment, it is convenient to measure the magnetic field in gauss keeping in mind that 10⁴ gauss is equal to one tesla. Using these units, $\mu_0/h = 1.3996$ MHz/gauss. The above equations are true as long as the energy levels are a linear function of the applied magnetic field. When terms quadratic in the magnetic field need to be considered, an expansion for the frequency can be used as shown in the next paragraph. At even higher fields, the full Breit-Rabi equation must be used.

To obtain an expression for the transition frequencies that is good to terms quadratic in the magnetic field, it is convenient to re-label the energy levels in terms of an average quantum number [2F-1]. The resonance frequencies for transitions between the levels |F, M> and |F, M-1> with energies W(F, M) and W(F, M-1) and mean azimuthal quantum number

$$\bar{M} = M - \frac{1}{2}$$

$$\omega_{FM} = (W_{F,M} - W_{F,M-1}) / \hbar \quad 2F-3$$

Physically meaningful values of \bar{M} occur in the range $-I \leq M \leq I$.

The resonance frequencies correct to second order in the magnetic field are given by

$$\omega_{I+1/2,\bar{M}} = \frac{B(g_J\mu_B - 2\mu_I)}{(2I+1)\hbar} - \frac{2B^2\bar{M}(g_J\mu_B + \mu_I/I)^2}{(2I+1)^2\hbar^2\omega_M} \quad 2F-4$$

$$\omega_{I-1/2,\bar{M}} = \frac{B(g_J\mu_B + 2\{I+1/I\}\mu_I)}{(2I+1)\hbar} + \frac{2B^2\bar{M}(g_J\mu_B + \mu_I/I)^2}{(2I+1)^2\hbar^2\omega_M} \quad 2F-5$$

where μ_B is the Bohr magneton and $\hbar\omega_M = (2I+1) A / 2$ is the energy splitting of the Zeeman multiplets at zero magnetic field. To first order in B , the resonance frequencies are independent of \bar{M} . To second order in B , the resonance frequencies exhibit a quadratic splitting proportional to $B^2 \bar{M}$ which is the same for both Zeeman multiplets [2F-2].

REFERENCES

- [2F-1] A. Ben-Amar Baranga et al, Phys. Rev. A, **58**, 2282 (1998).
- [2F-2] H. Kopfermann, "Nuclear Moments" (Academic Press, NY, 1958).

2G. Transient Effects

Up until now we have been considering optical pumping only in the steady state, either when the RF has been on for a relatively long time or when there is thermodynamic equilibrium. We will now consider transient phenomena.

We referred, in section 2D, to the time it takes to establish equilibrium after the pumping radiation has been turned on. Here, we will consider the behavior of the pumped system when the RF is rapidly turned off and on while tuned to the center of resonance. In the Zeeman region, at weak magnetic fields, the resonance frequency is given by

$$\omega_0 = 2\pi\nu_0 = g_f \frac{\mu_0}{\hbar} B_0 \quad 2G-1$$

The Gyromagnetic Ratio γ is defined as

$$\gamma = g_f \frac{\mu_0}{\hbar} \quad 2G-2$$

The Larmor frequency ω_0 is given by

$$\omega_0 = \gamma B_0 \quad 2G-3$$

Thus γ is the atomic equivalent of the gyromagnetic ratio used in nuclear magnetic resonance.

Figure 2G-1 shows a vector diagram of the spin and the magnetic fields that are relevant to this experiment. The vector B_{RF} represents the applied RF magnetic field that is provided by the coils at right angles to the static field. We will assume that the magnitude of the RF magnetic field is always much smaller than that of the static field. We will also consider the problem classically.



FIGURE 2G-1. \mathbf{F} and its precession about \mathbf{B} . \mathbf{B}_{RF} is the RF magnetic field.

Consider the system as seen in a coordinate system that is rotating about \mathbf{B} . The equation of motion is

$$\frac{d\mathbf{F}}{dt} = \gamma \mathbf{F} \times \mathbf{B} \quad 2G4$$

The oscillating magnetic field can be considered to consist of two counter-rotating magnetic fields, and transformed to a coordinate system rotating about \mathbf{B} with angular frequency ω . Then

$$\frac{d\mathbf{F}}{dt} = \frac{\partial \mathbf{F}}{\partial t} + \omega \times \mathbf{F} \quad 2G5$$

or

$$\frac{\partial \mathbf{F}}{\partial t} = \gamma \mathbf{F} \times \mathbf{B} + \mathbf{F} \times \omega = \gamma \mathbf{F} \times (\mathbf{B} + \frac{\omega}{\gamma}) \quad 2G6$$

$$= \gamma \mathbf{F} \times \mathbf{B}_{\text{eff}} \quad 2G7$$

where

$$\mathbf{B}_{\text{eff}} = \mathbf{B} + \frac{\omega}{\gamma} \quad 2G8$$

In the rotating frame, the effect is the addition of a magnetic field $\frac{\omega}{\gamma}$ to the dc field \mathbf{B} . [2F-1]

Consider the RF field to be composed of two counter-rotating components of which one has an angular velocity of $-\omega$ as shown in Figure 2G-2. The effective magnetic field is given by [2G-2]

$$|\mathbf{B}_{\text{eff}}| = \left[(B - \frac{\omega}{\gamma})^2 + H_{rf}^2 \right]^{\frac{1}{2}} = \frac{|a|}{|\gamma|} \quad 2G9$$

where $a = \left[(\omega_0 - \omega)^2 + (\gamma B_{rf})^2 \right]^{\frac{1}{2}} = \left[(\omega_0 - \omega)^2 + \left(\frac{\omega_0 B_{rf}}{B} \right)^2 \right]^{\frac{1}{2}}$

and $\omega_0 = \gamma B_0, \quad \cos\theta = \frac{\omega_0 - \omega}{a}$

At resonance $\omega = \omega_0, \cos\theta = 0$ and $\theta = 90^\circ$.

Also $a = \frac{\omega_0 B_{rf}}{B}$ and $|\mathbf{B}_{\text{eff}}| = \frac{\omega_0 B_{rf}}{\gamma B} = \gamma B \cdot \frac{B_{rf}}{\gamma B} = B_{rf}$.

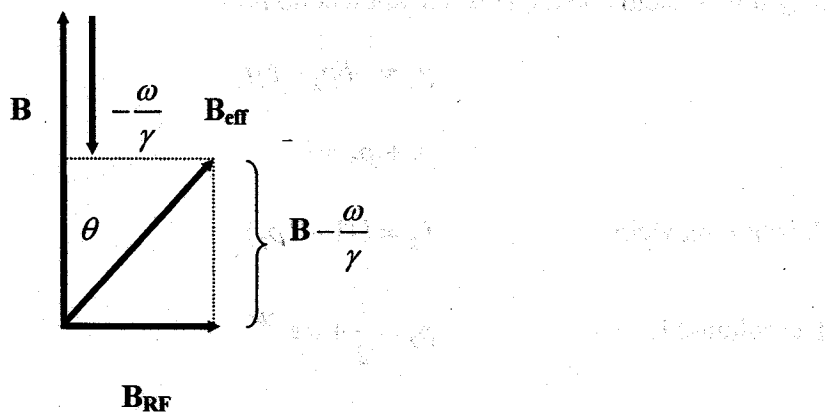


FIGURE 2G-2. Magnetic fields in the rotating coordinate system.

At resonance in the rotating frame, \mathbf{F} precesses at the Larmor frequency about $\mathbf{B}_{RF} = \mathbf{B}_{eff}$. Off resonance, it precesses about \mathbf{B}_{eff} . This precession is equivalent to a change in the quantum number M , or a transition between the M sublevels. At resonance, the Larmor frequency is $v = \gamma B_{eff}$ resulting in a period of $T = 1/\gamma B_{eff}$. At a given value of the RF

magnetic field, the ratio of the periods of the two isotopes is $\frac{T_{87}}{T_{85}} = \frac{\gamma_{85}}{\gamma_{87}}$. In the present experiment we will only be interested in the situation at resonance.

Assume that the optical pumping has created an excess population in the $M = 2$ sublevel in the absence of RF. To the approximation used here we will consider only the $M = 2$ and $M = 1$ sublevels, and neglect all effects of collisional relaxation. Assume now that the RF is applied at the resonance frequency. The situation is as depicted in Figure 2G-3.

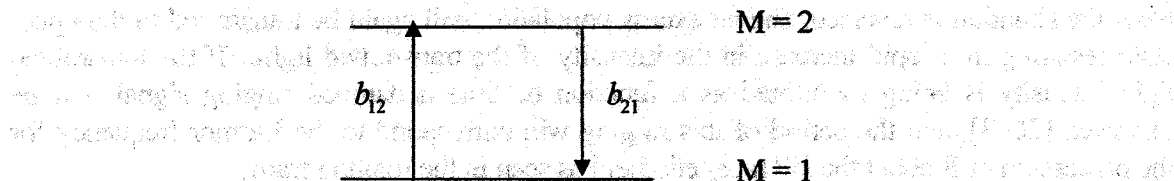


FIGURE 2G-3. RF transitions between the $M = 2$ and the $M = 1$ sublevels.

The arrows labeled b_{12} and b_{21} represent the transition probabilities from the $M = 1$ to the $M = 2$ and the $M = 2$ to the $M = 1$ sublevels respectively. The rate equations are

$$\dot{p}_2 = -b_{21}p_2 + b_{12}p_1 \quad 2G-12$$

$$\dot{p}_1 = -b_{12}p_1 + b_{21}p_2$$

However, $b_{12} = b_{21} = b$. The equations are not independent, and therefore we will consider only one of them and the normalization condition.

$$\dot{p}_2 = -bp_2 + bp_1$$

2G-13

$$p_1 + p_2 = 1$$

Substitution yields

$$\dot{p}_2 = b(1 - 2p_2)$$

2G-14

The solution is

$$p_2 = \frac{1}{2} + \delta e^{-2bt}$$

2G-15

$$p_1 = \frac{1}{2} - \delta e^{-2bt}$$

where δ represents the initial excess population in p_2 . At $t = 0$ $p_2 = 1/2 + \delta$ and approaches $1/2$ at $t = \infty$. Similarly $p_1 = 1/2 - \delta$ at $t = 0$ and approaches $1/2$ at $t = \infty$. Thus the effect of the RF is to equalize the population of the two states. δ depends on the intensity of the optical pumping radiation and b is proportional to the current in the RF coils.

The above calculation suggests an exponential approach to the equal population condition. The situation is different, however, if the RF is suddenly turned on at the resonance frequency after the optically pumped equilibrium has been attained. Since the transition probability is the same for the up or down transition, and the initial population of the upper state is greater than that of the lower, the number of downward transitions will be greater than that of the upward and excess population will be created in the lower state. This will result in a rapid decrease in the intensity of the transmitted light.

Now the situation is reversed, and an excess population will again be transferred to the upper state resulting in a rapid increase in the intensity of the transmitted light. If the transmitted light intensity is being monitored as a function of time a damped ringing signal will be observed [2G-3], and the period of this ringing will correspond to the Larmor frequency for the precession of F about the RF magnetic field as seen in the rotating frame.

The above treatment neglects the effects of the other magnetic sublevels and also the effects of collisions between rubidium atoms and collisions between rubidium atoms and the buffer gas. However, the basic properties of the observed signal are described.

Before the RF is applied the initial population of the p_2 state is $\frac{1}{2} + \delta$. The time to reach $1/e$ of this value can be shown to be

$$t_{1/e} = \frac{1}{2b}$$

2G-16

Thus this time is inversely proportional to the RF perturbation and to the current flowing in the RF coils. It is instructive to measure this time as a function of the RF current.

REFERENCES

- [2G-1] I. I. Rabi, N. F. Ramsey, and J. Schwinger, Rev. Mod. Phys. **26**, 167 (1954).
- [2G-2] N. F. Ramsey, "Molecular Beams" (Oxford University Press, London, 1969).
- [2G-3] G. W. Series, Rept. Progr. Phys. **22**, 280 (1959).

3. APPARATUS

The specifications given here are not meant as a guarantee of performance, but as typical values. We expect individual instruments to vary, however if some value is more than a factor of two different from those given, this should be brought to the attention of Teachspin Inc.

3A. Rubidium Discharge Lamp

The Rubidium discharge lamp consists of an RF oscillator, oven and gas bulb. The gas bulb is filled with a little Rubidium metal and a buffer gas. The bulb sits within the coil of the oscillator (Figure 3A-1). Stray ions within the bulb are accelerated by the RF electric fields caused by changing magnetic fields. Collisions between the accelerated ions and neutral atoms (both buffer gas atoms and vaporized Rb atoms) cause those atoms to be either ionized or to enter into an excited electronic state. Relaxation of the excited state by spontaneous emission results in the observed resonant radiation from the lamp. The bulb is heated in the oven to increase the Rb vapor pressure (see vapor pressure curves in theory section), and also to regulate the lamp temperature. The lamp intensity changes rapidly with temperature, increasing by 5%/ $^{\circ}\text{C}$ at operating temperatures. The oven temperature is set to $115\ ^{\circ}\text{C} \pm 5\ ^{\circ}\text{C}$.

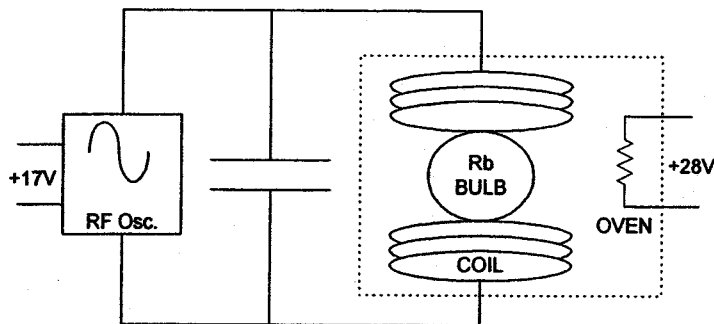
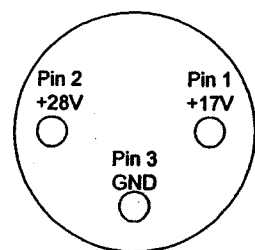


Figure 3A-1. a) Discharge Lamp



b.) Back Panel Lamp Connections

The rubidium bulb has been isotopically enriched with Rb^{87} . It is filled with 50% Rb^{87} and 50% natural Rb. This equates to about 36% Rb^{85} and 64% Rb^{87} . The buffer gas is Xenon. This lamp is an optically extended source of light with radiation from both isotopes of Rubidium and multiple lines from the buffer gas Xenon.

| | |
|-----------------------------|---------------------------------------|
| Oscillator Voltage | +17 V DC |
| Oscillator Current | 120-160 mA |
| Oven Voltage | +28V DC |
| Oven Current | 450 mA (Warm-up) 100mA (Steady-state) |
| Oscillator Frequency | 75-90 MHz. |
| Oven Temperature | 115 ± 5 °C |
| Lamp Intensity ¹ | all lines 9.0 µW 795 nm 1.7 µW |

The electrical connections to the lamp are made at the back panel. The lamp uses +17 VDC for the oscillator and +28 VDC for the oven. The connection looking into the back panel socket is shown in Figure 3A-1. The Lamp oscillator, oven, and the experimental cell temperature controller all run off a separate +28V power supply.

Voltage is supplied to the lamp when the main power is turned on. Within a few minutes of applying power to the lamp you should see the pinkish discharge light. The oven within the lamp takes 10 to 20 minutes to stabilize. *It should be noted that the 795 nm spectral line that is used in the experiment is in the near infrared and cannot be seen by the human eye. The light that you see comes from other lines of Rubidium and Xenon.*

¹ The Lamp Intensity is measured by the photodiode. The photodiode was placed such that the front face of the photodiode was 15 cm. from the front face of the lamp and the diode adjusted vertically for a maximum signal. We use the specified responsivity of the diode as 0.6 A/W. For the single 795 nm line measurement the interference filter was placed between the lamp and diode, we assumed the transmission coefficient of the interference to be 0.80 (See figure 3C-1)

3B. Detector

The detector is a Silicon photodiode from Photonic Detectors Inc. PDB-C108 (See spec sheet (Appendix A) The active area of the diode is circular, with a diameter of $\frac{1}{4}$ inch. The spectral response at 795 nm is about 0.6 A/W. The diode is connected to a current to voltage preamplifier. (See Figure 3B-1) To determine the current supplied by the photodiode, divide the output voltage by the "gain" resistance. The diode is used in photovoltaic mode (cathode grounded, rather than reversed biased) for minimum noise. The preamp is a current-to-voltage converter with three "gain" settings selectable by the small switch on the front of the detector. It has a two-pole low-pass filter to roll off the high frequency gain at about 10kHz.(see Table 3B-1). The photodiode preamplifier has a voltage output of 0.0 to -11.5 V. ***It is important that the pre-amp be operated at a gain setting such that the output is between -2.0 to -8.0 V to avoid saturating the pre-amp.*** Power connections to the preamp are by the black plastic connector to the front panel of the electronics box.

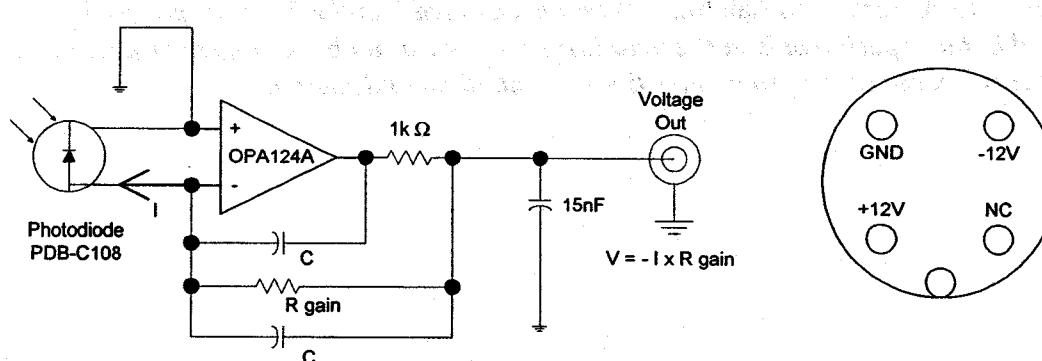


Figure 3B-1. a.) Schematic of Photodiode Preamplifier. b.) Preamp Power Connections

| Gain Resistor (MΩ) ± 5% | Low pass 3dB point (kHz.) ± 10% | Noise ² (μV _{p-p}) |
|----------------------------|------------------------------------|--|
| 1 | 12.0 | 20 |
| 3 | 8.0 | 40 |
| 10 | 5.0 | 100 |

Table 3B-1. Photodiode Preamplifier Specifications

The signal from the preamp is on the Coax cable with BNC connector labeled Detector. This separate detector connector allows the student to observe the signal from the preamp directly on an oscilloscope. Note: the signal from the preamp is negative with respect to ground.

Normally the preamplifier output will be plugged into the input of the detector section of the electronics box. ***The detector inverts the signal from the preamp so that more light appears***

² Peak to peak noise voltage measured with the front of photodiode covered and with a bandwidth of 0.1 Hz to 1 kHz. (Detector electronics: gain = 1000, Low-pass time constant = 1ms, 10s oscilloscope trace)

as a larger voltage on the meter or detector output. The detector electronics consist of the follow sections:

DC Offset: 0 -10 V DC Set by ten turn potentiometer and fine control approximately 0-20mV set by a one turn potentiometer. The fine control will only be useful at the highest gain settings.

Gain: 1,2,5...100 Adjustable gain set by selector switch and X1, X10 set by toggle switch. Maximum gain is 1000.

Low Pass Filter: A two pole low pass filter with the following time constants; min., 1ms, 10ms, 100ms, 1s, 3s. When set to min. the frequency response is determined by the gain setting of the preamplifier

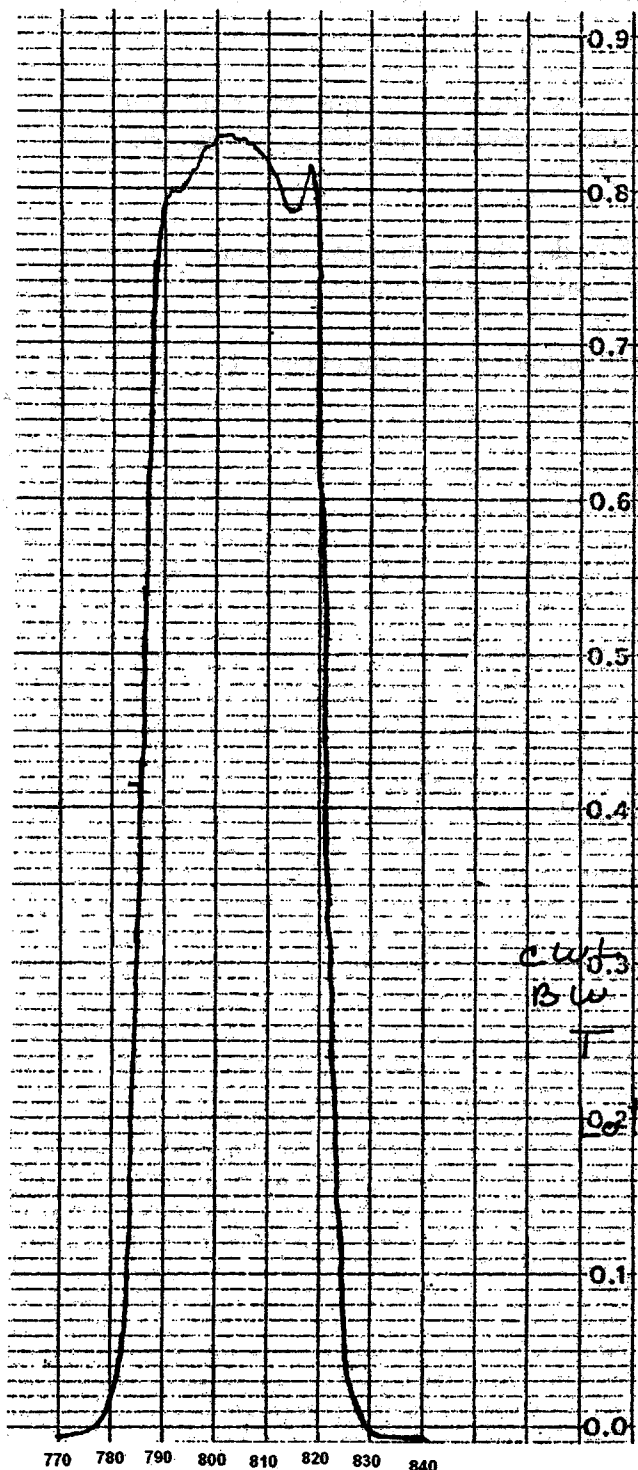
Meter: The meter displays the output voltage of the detector electronics. The range is -4 to +4 volts with the meter multiplier toggle set to X1 and -8 to +8 Volts when set to X2.

There is 80 μ V_{p-p} (referred to the input) of 60 cycle pickup noise on the detector output.

3C. Optics

Two plano-convex lenses: Diameter 50mm, focal length 50mm. Plano-convex lenses minimize spherical aberrations when there are large differences in the object and image distance from the lens. For best use, the curved side should face towards the larger distance.

(See Figure 3-1)



Interference filter: Diameter 50mm. The transmission characteristics of the filter are shown in Figure 3C-1. We are mostly interested in the Rubidium D lines at 780nm and 795 nm. The transmission peak of the interference filter may be "tuned" to shorter wavelengths by rotation about the vertical axis. If λ_0 is the peak wavelength then when the filter is tilted at an angle θ the new peak wave length will be given by,

$$\lambda_s = \lambda_0 (1 - \sin^2 \theta / n^2)^{1/2}$$

(Building Scientific Apparatus, Moore, Davis, and Coplan; Addison-Wesley Second edition pg. 166) where n is the index of refraction of the filter.

Two Linear Polarizers in Rotatable Mounts: Diameter 50mm. Figure 2C-2 shows the transmission and extinction characteristics of the polarizers. The linear polarizer mount has a alignment mark indicating the axis of polarization. The mark should be accurate to $\pm 5^\circ$. *The rotatable mounts are only held in place by the thumb screw and if the thumb screw is not tighten it is possible for the polarizers or quarter wave plate to fall out.*

Figure 3C-1 Transmission of Interference Filter

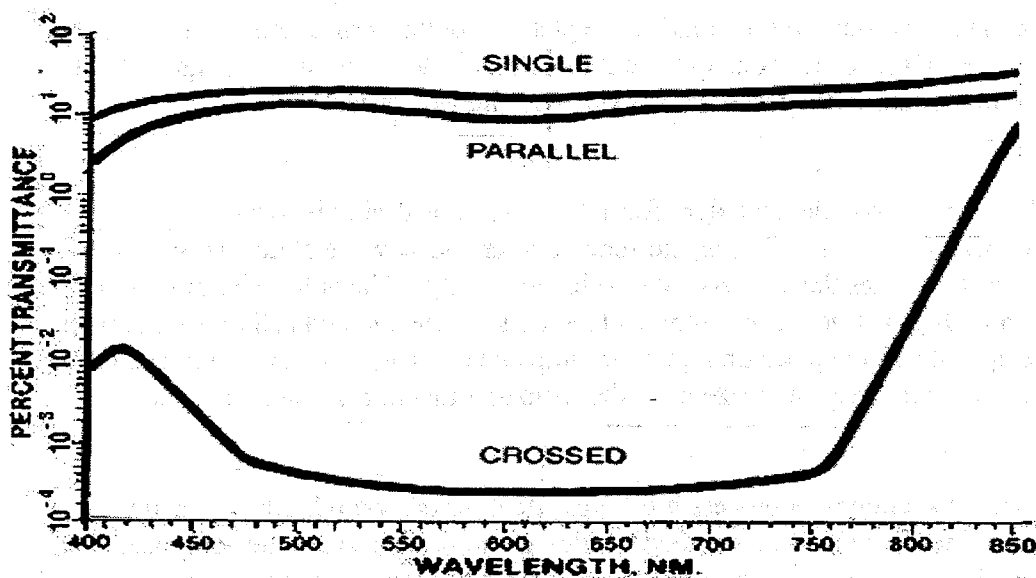


Figure 3C-2. Transmission Characteristics of Linear Polarizers

Quarter Wavelength Plate in Rotatable Mount. Diameter 50 mm, "optical thickness" 205 ± 5 nm. When properly oriented, the quarter wave plate allows linearly polarized light to be converted to circularly polarized light. The plate has two optical axes (at 90 degrees to each other) with different indices of refraction along each axis. Light travels at different speeds along each axis. The axes are called the "fast axis" and "slow axis". To produce

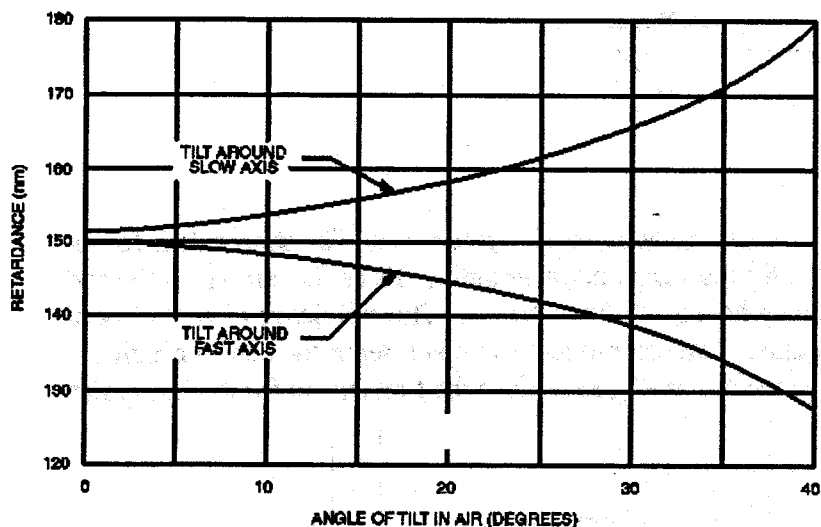


Figure 3C-3 Tilt Tuning o Quarter Wave Plate.

circularly polarized light, monochromatic linear polarized light is placed incident to the plate at 45° to each axis. If the plate is of the correct thickness, then the phase lag along the slow axis causes the light exiting the plate to be circular polarized. The "optical thickness" of the plate may not be $795\text{nm}/4$ which is the desired value. Tuning the optical thickness

(retardation) can be accomplished by rotating the plate about the vertical axis. Rotation about the slow axis increase the retardation, and about the fast axis decreases it. See figure 3C-3. This tuning method requires the fast or slow axis to be aligned vertical.

Alignment:

The first lens is used to collect the light from the lamp. It is desirable to have approximately parallel light rays for the interference filter and $\frac{1}{4}$ -wave plate. However, the extended source size makes this impossible to achieve exactly. The bulb in lamp is approx. 10 mm X 15 mm. It is instructive to remove all the optics, detector, and cell (see section on cell) from the optical rail and place on it just the lamp and one lens. Then in a darkened room, one can observe the spot shape and size from the lamp as a function of the lamp lens separation.

During most of the alignment process it is helpful to have the room lights dimmed to reduce stray light interference. You do need a little light to be able to see the components and detector meter. The optics can be rotated both about the z-axis (the direction along the optical rail) and the vertical axis (towards the center of the Earth) in the alignment process. The experimental cell has been centered 3.5" above the optical rail. (3.5" is also the length of a standard business card which we have found useful for alignment.)

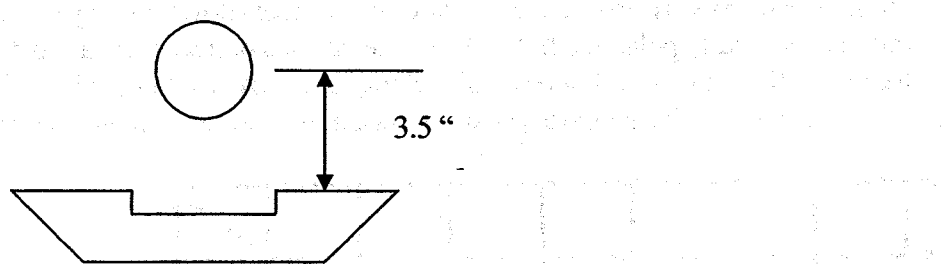


Figure 3D-1

Note that the magnet coils are NOT centered on the optical rail. The short side is for the detector and the longer side is for the lamp and other optics. Place the lamp near the end of the optical rail with the center hole 3.5" above the rail. This will leave plenty of room for the other optical components. You can move the lamp closer to the cell (for higher light intensity) once you have the optics aligned. Place the first lens in front of lamp flat

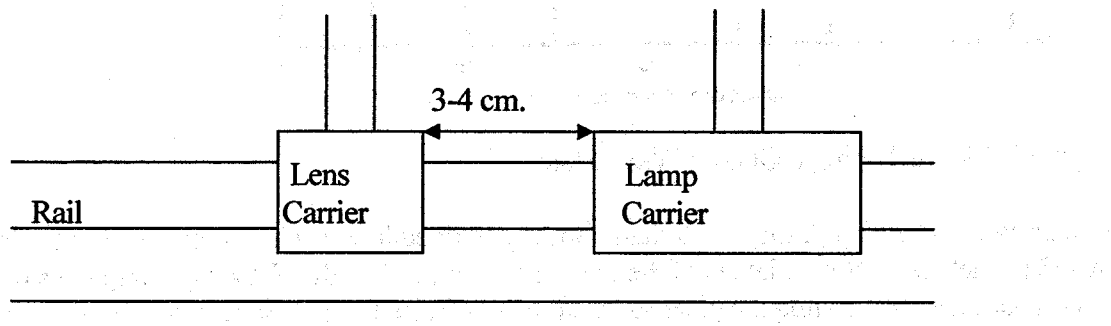


Figure 3C-2 Side View of Optical Rail.

side towards the lamp, so that the distance between the center of the lamp and center of the lens about 5 cm, this corresponds to a distance of 3-4 cm. between the carriers on the rail. You will see that one side of the optical rail has a ruler attached. Place the second lens and the detector on the short side of the optical rail. The separation between the lens and detector carriers should be about 1-2 cm. The flat side of the lens should face the detector and the detector should be centered at 3.5" above the rail.

Turn on the electronics (See electronics section), making sure that the lamp and detector are plugged in. After a few minutes the lamp should turn on and in about 15 minutes the lamp will be stable.

- 1) Set the cell temperature to 20 °C {This is not a critical step. We just don't want the cell temperature to be set at some high temperature were there is very little transmission. If the cell is set at any temperature below 50 °C that should be fine.} Set the gain and offset of the detector electronics to zero.
- 2) Set the preamp "gain" to $1M\Omega$ (switch down). The meter should be reading off scale (too much light for the preamp.)
- 3) Put the interferences filter on the rail to reduce all but the 795 nm. Rb line {Though it makes little difference in this case, the reflective side of the interference filter should be placed towards the light source.}
- 4) Now adjust the position and height of the lenses for a maximum light signal. Since you set the height of the detector and lamp to 3.5", the height of the cell, you should not change these heights.

Alignment of Polarizers:

The alignment marks on the linear and circular polarizers are accurate to $\pm 5^\circ$. The $\frac{1}{4}$ -wavelength retarder may not be of exactly the right thickness. Careful alignment of these components can improve your signals by as much as 30%. However this is not necessary to get a signal. For a quick alignment, set the linear polarizer at 45° and the $\frac{1}{4}$ -wave plate at 0° or 90° . ***The light needs to go through the linear polarizer before it passes through the $\frac{1}{4}$ -wave plate.***

For a better alignment, set the first linear polarizer at 45° . Set the second linear polarizer in front of the detector and rotate it about the z-axis till you see maximum extinction, minimum signal. Typical extinction is about 2% of the maximum signal. The alignment mark on the second polarizer should be close to 135° or 315° . (90° difference from first polarizer) Now place the $\frac{1}{4}$ wave plate after the first polarizer and rotate the wave plate about the z-axis till you see a maximum signal. The alignment mark should be near $0, 90, 180$, or 270° . You may now rotate the second linear polarizer about the z-axis, (using it as an analyzer) to determine the degree of circular polarization.

For complete Circular polarization there should be no change in the signal level as you rotate the linear polarizer. Typical changes from maximum to minimum are between 0% to 50%. If there is a change in light level reaching the detector as you rotate the second linear polarizer, then you can "tune" the $\frac{1}{4}$ -wave plate by rotation about the fast or slow axis (Figure 3E-1) Rotate the $\frac{1}{4}$ -wave plate slightly (5-10°) about the vertical axis. Now rotate the second linear polarizer again and observe the relative changes in the signal. If the relative change is worse than before, then the $\frac{1}{4}$ -wave plate needs to be rotated 90° about the z-axis. Otherwise continue tilting the $\frac{1}{4}$ -wave plate about the vertical axis and analyzing the result with the second linear polarizer.

For the absolute best in alignment (given the components available) one needs to correct for the slight differences between the alignment marks and the real position of the axes. There are several ways to do this. The way we choose to do this is by adjusting the first linear polarizer to 45°. We do this by observing that at exactly 45° a rotation of 180° about the vertical axis is equivalent to a rotation of 90° about the z-axis.

Remove the circular polarizer and have in place only the two linear polarizers. Set the first LP for 45°. Rotate the second LP about the z-axis until you observe the minimum signal. Record the position of the second linear polarizer. Now flip the first LP (rotate 180° about vertical axis). Again rotate the second LP about the z-axis until you observe the minimum signal. Record the position of the second LP. If the difference in position from the first reading is 90° then the first LP is at 45° to the vertical. If the difference is less than 90°, then increase the setting of the first LP by a few degrees (the amount you need to change it is exactly $\frac{1}{2}$ the difference between your readings of the second LP and 90°).

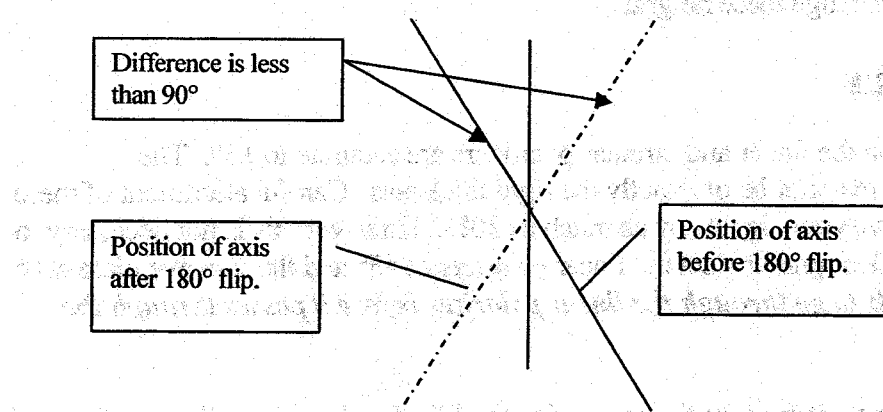


Figure 3C-1

If the difference is greater than 90° then you need to decrease the angle of the first LP. After the first LP is set to 45° then follow the previous steps for alignment of the $\frac{1}{4}$ -wave plate.

3D. Temperature Regulation

The following components make up the cell temperature regulation system.

Temperature regulator: Proportional, Integral, Derivate (PID) temperature controller with associated electronics.

Temperature probe: Type T (Copper – Constantan) Thermocouple (5 μm wire)
{Constantan is magnetic and the small wire size was chosen such that the magnetic effects of the probe were unobservable, but the small wire size also makes the probe very delicate.}

Oven: The oven contains the following:

Rubidium cell: Glass cylinder with an outside length of 36mm and outside diameter of 25 mm. the wall thickness is about 1.5 mm. The cell contains rubidium metal with associated vapor and 30 torr of neon as a buffer gas.

Cell holder: Foam insert that holds the cell in the center of the oven.

Heater: The heater is an open ended glass cylinder on which is wrapped non-magnetic bifilar wound heater wire. The resistance of the heater is about 50Ω .

Insulation: A layer of foam insulation surrounds the heater.

Oven casing: The oven casing is a Plexiglas cylinder. The removable end caps contain 50mm optical windows. Holes in the casing allow for the heater wire and thermocouple wire to enter the inside of the oven. Also, attached to the oven casing and RF wiring box (to be discussed in the RF section)

Operation:

The thermocouple plugs into the front panel blue plug. The heater is connected to the blue banana plugs on the front panel. The manual for the controller has been included. There are three keys on the controller which are used to program it, (Figure 3D-1) the SCROLL, UP and DOWN keys. Under normal operation you will only be changing the temperature set-point. The controller will normally display the current temperature (PROC). Press the SCROLL key once and the parameter name will appear, wait 1.5 seconds and the parameter value will appear. Press the SCROLL key twice and the controller will step to the next parameter name SP (Set Point), wait 1.5 seconds and the value of the set point will be displayed. You may change the value of the set point with the UP and DOWN keys. To get back to the current temperature press the SCROLL key twice again. The temperature is displayed in degrees Celsius.

The minimum temperature is set by the ambient room temperature. The maximum temperature of about 100 °C. is power limited by the power supply 28V and the heater

resistance 50 ohm. There is no need to worry about your students burning out the heater. There is simply not enough power to raise the temperature significantly above 100 °C.

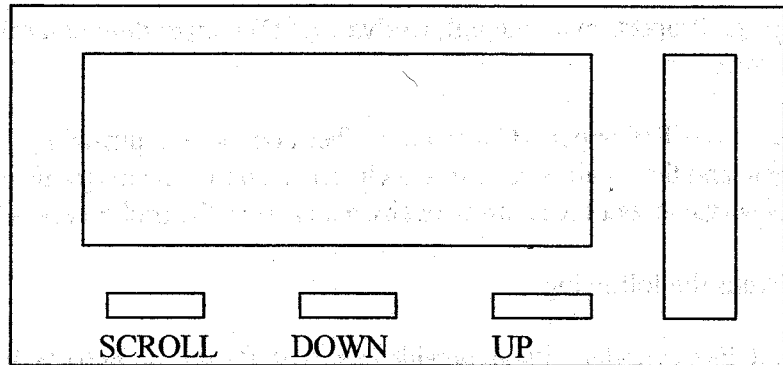


Figure 3D-1

Instrument Configuration and Control Setup of the controller has been done by Teachspin. The Instrument Configuration is as follows: (Please refer to the Controller Manual if you have questions).

To enter the Instrument Configuration mode press and hold the SCROLL and UP keys simultaneously until the display begins to flash. When the display begins to flash release the SCROLL and UP keys and press the DOWN key. The SCROLL key is used to step through the parameter sequence. (See page 13 of the Controller manual). First the parameter name is displayed on the screen, after 1.5 seconds of no key activity the parameter value is displayed. The UP and DOWN keys are used to change the parameter value. Pressing the SCROLL key returns you to the parameter name, pressing the SCROLL key again steps you to the next parameter name. To exit the Instrument Configuration mode, press and hold the UP and Down keys simultaneously.

Note: When exiting the mode the parameter name must be displayed and not the parameter value!

Though not discussed in the Controller manual, we have found that changing the Instrument Configuration also resets the Control Set-up parameters to their default values. If you do make changes to the Instrument Configuration, you will also have to change the Control Setup.

INSTRUMENT CONFIGURATION PARAMTERS

| | | |
|------|-------|---|
| SEnS | 210 | Sensor Select (Type T thermo couple, high resolution, °C) |
| rLO | 10.0 | Input Range Minimum |
| rHi | 130.0 | Input Range Maximum |
| OUtS | 0.200 | Output Select (DC pulse, No alarm, No option) |
| SPS | 1 | Single/Dual Setpoint, Select (one set point) |
| CntL | rPd | Control Select (Reverse-acting PID) |
| tunE | EASY | Tuning Select (Easy tune) |

There have also been changes made to the Control Setup, some of these variables (indicated with an asterisk *) only appear if the Controller is in Manual tuning mode. To enter the Control Setup mode press and hold the UP and DOWN keys simultaneously. The same key action exits this mode. Note: When exiting the mode, the parameter name must be displayed and not the parameter value!

CONTROLLER SETUP PARAMETERS

| | | | |
|------|------|----------------------------|-----------------|
| SP | 50.0 | Set Point | °C |
| Pb | 5.8 | Proportional Band* | % |
| rSET | 8.41 | Reset (Integral) value* | minutes.seconds |
| rAtE | 1.26 | Rate (Derivative) value* | minutes.seconds |
| biAS | 0.0 | Bias (manual Reset) value* | % |
| FiLt | 30 | Filter Time Constant | seconds |
| OFFS | 0 | Input Ofset | |
| Ct | 0.5 | Output Cycle Time | seconds |
| SPL | OFF | Set Point Lock | |

We have chosen to set up the PID controller in Easy Tune mode.³ This mode offers satisfactory performance and all the experimenter has to do to change the temperature is change the set point. Though we have not done any careful studies, we have observed more stable signals when the controller is in manual tuning mode *and is tuned correctly!* The problem with the manual tuning mode is that optimal tuning parameters at one temperature will be different from those at another temperature

There are several ways to tune the controller. First we use a list of tuning parameters for several different temperatures (Appendix B). The second is the Pretune Manual mode (see page 21 of the Controller Manual.). To use pretune, first put the controller in manual tuning, then change the set point by 10 °C, then select the process variable display. While the name PROC is on the display press and hold the UP key. PROC will start to blink, when the decimal point and the right hand side of the displays begins to blink then Pre-Tune is active and you can release the key.

³ The tuning of PID controllers (choosing the right mix of P, I and D) is an active area of engineering and the interested student is encouraged to research it on their own.

Finally there is a vast engineering literature on PID controllers (search the web under tuning +"PID controller"). A student who feels more comfortable with engineering than with the Wigner-Eckhart Theorem might enjoy determining the tuning parameters themselves. We have used the Ziegler-Nichols Closed Loop Tuning Method with some success. The controller temperature display does not have enough resolution to display the small thermal oscillations, used in this method to determine the tuning parameters, so we monitored either the voltage going to the heater (by putting a voltmeter across the banana plugs of the electronic box) or by monitoring the oscillating light level through the rubidium cell. In either case it would be useful to have a strip chart recorder or computer with an Analog to Digital Converter to monitor the slow oscillations (periods of several minutes).

Temperature Electronics:

The dc pulse output from the Temperature Controller is passed through a low pass filter ($\tau = 10\text{s.}$) and then amplified. The out put on the blue banana plugs is a DC voltage from 0 – 26V with a slight 2 Hz ripple. The 2 Hz. ripple is from the 0.5 second cycle time of the DC pulse output.

3E. Magnetic Fields

All DC magnetic fields are produced by Helmholtz coil pairs. The coils are copper wire wrapped on phenolic bobbins. The following table lists their properties:

| | Mean Radius cm(inches) | Turns/Side | Field/Amp (T x 10 ⁻⁴ /Amp) | Maximum Field (T x 10 ⁻⁴) |
|---------------------|---------------------------|------------|--|--|
| Vertical Field | 11.735 (4.620) | 20 | 1.5 | 1.5 |
| Horizontal Field | 15.79 (6.217) | 154 | 8.8 | 22.0 |
| Sweep Field | 16.39 (6.454) | 11 | 0.60 | 0.60 |

Table 3E-1 Magnetic Field values. The calibration of Field/Amp is only approximate. The student will have to determine a more accurate value.

A simplified schematic of the current regulated field control circuitry is shown in Figure 2E-1. The circuit is a simple voltage-to-current converter. The Reference Voltage determines the voltage across the sense resistor and hence the current through the coils. The compensating network "tunes" out the coil inductance so that it appears as a pure resistance to the rest of the circuit. The compensating network draws no DC current.

The voltage across the sense resistor may be measured via tip jacks. The 100 ohms is in series so that the sense resistor can not be accidentally shorted by the student. Connections to the coils are made by the front panel banana plugs. **All the field controls are "unipolar".** If you wish to reverse the field direction you must switch the front panel banana jacks.

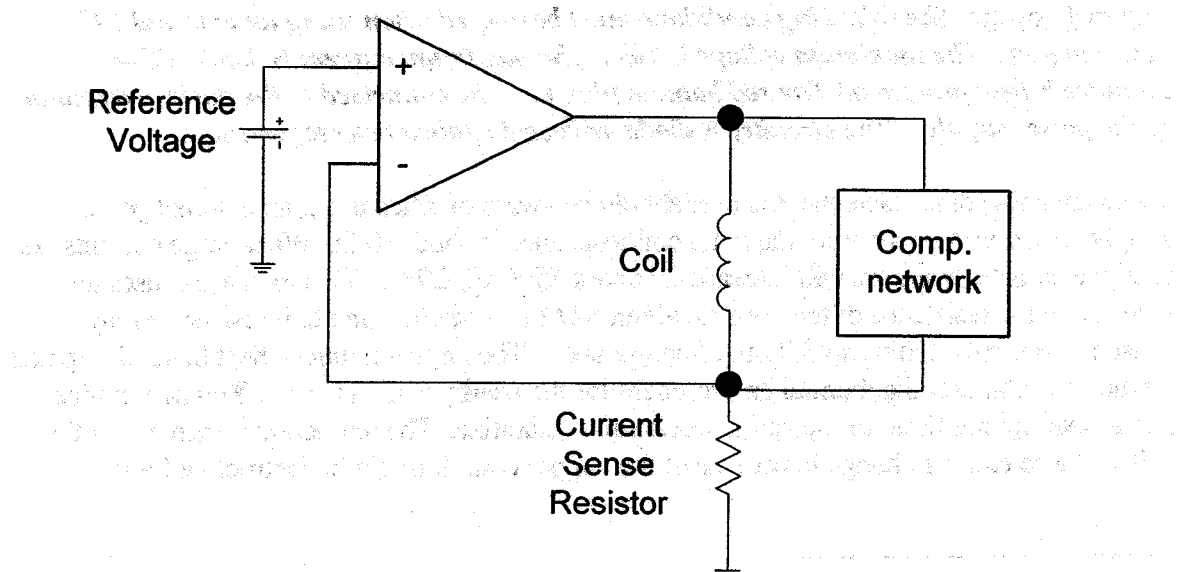


Figure 3.E-1). Schematic of Filed control circuitry.

Vertical Field. The Vertical Field is run between ground and the negative supply voltage. This is done because of the current limit of the power supply. The sense resistor is thus at -15V with respect to ground. ***Caution should thus be exercised if this voltage is monitored with anything but a floating voltmeter.***

Sense Resistor: 1Ω , 1%. Monitoring of the sense resistor is done through the back panel tip jacks.

Polarity: The vertical coil is wired so that field will point downward when the red jack is in the red plug. This is the correct direction to cancel the Earth's Field in the Northern hemisphere. If you are in the Southern hemisphere you should reverse the jacks. A current of about 0.33 Amperes will cancel the vertical field in Buffalo, NY. USA.

Control: The ten turn potentiometer sets the Reference Voltage. The maximum voltage is 1.0 Volt. (one turn = 0.1 Volt = 0.1 Ampere.)

Horizontal Field. The Main Horizontal Field can be run off the internal power supply with a maximum current of about 1.0 Ampere. Or an external power supply can be used to go to higher fields. The external power supply is connected to banana plugs on the back panel. A toggle switch on the back panel determines which supply is in use.

Sense Resistor: 0.5Ω , 1%. Monitoring of the sense resistor is done via front panel tip jacks.

Polarity: The Horizontal Field is wired such that the field will point from the lamp towards the detector (in the direction of light propagation) when the red plug is in the red jack.

Control: The ten turn potentiometer sets the Reference Voltage. The maximum voltage is 1.5 Volt. (one turn = 0.15 Volt = 0.3 Ampere.)

External Power: *The following conditions must be obeyed when using an external DC power supply. The maximum voltage is 40V. The maximum current is 3.0 A. (The circuitry is fuse protected.) The red banana plug must be connected to the positive terminal of the power supply. (The circuitry is diode protected against reverse polarity.)*

There are a few other facts that the user should be aware of when using an external power supply. At room temperature, the main coil resistance is about 10Ω . When large currents are used the coils temperature will increase (to about 75°C @ 2.7A). This increase causes an increase in the resistance of the coils (to about 12Ω).⁴ The changing coil resistance may cause the control circuitry to fall out of compliance. The large amount of heat being dissipated by the coils changes the thermal environment for the nearby cell and lamp. You may notice that it takes a long time for the cell temperature to stabilize. The temperature increase of the coil will also cause a change in the size of the copper coil. It might be instructive for the

⁴ Because we are using a current regulated supply there is a little positive feed back in this situation. As the temperature increases the resistance also increases, but this causes more power to be delivered to the coils (I^2R) which further increases the temperature, thus eliminating the current.

students to estimate the magnitude and sign of this change to determine if it would have any effect on their field calibration.

Error light: The error light will come on when the current regulated supply is close to being out of compliance (not enough voltage to supply the desired current). For efficient operation when using an external power supply the voltage of the external power supply should be set a few volts above the point where the error light comes on. The pass element of the control circuitry (which is the power transistor mounted on the back panel heatsink) must dissipate all the excess power. In the worst case scenario the pass transistor will warm up to 90 °C.⁵ This is within transistor's specifications, but it will be happier and live a longer life if it is kept cooler.

Horizontal Sweep Field. We often refer to this field as just the Sweep field. The Sweep field coil is a single layer of wire wrapped on top of the Horizontal field coils.

Sense Resistor: 1.0 Ω, 1%. Monitoring of the sense resistor is done via front panel tip jacks.

Polarity: The Sweep Field is wired such that the field will point from the lamp towards the detector (in the direction of light propagation) when the red plug is in the red jack.

Control: The Reference Voltage for the sweep field is the sum of three voltages; a Start Field voltage, a Sweep voltage, and a Modulation voltage. We will discuss each in turn. The maximum current that the sweep control can supply is about 1.0 A. When turned to full scale both the Start field and Sweep (Range) voltage are about 1.0 V. This means that it is very easy to set the sweep control so that it is out of compliance. ***There is no error light to warn the students when this happens.*** They need to be alert to the possibility.

Start Field: The ten turn potentiometer sets the Start Field voltage. The maximum voltage is about 1.0 Volt. (one turn ≈ 0.1 Volt = 0.1 Ampere.)

Sweep Field: The Sweep voltage is a voltage ramp that starts at zero volts and goes to the voltage set by the ten turn potentiometer marked Range. The maximum range voltage is about 1.0 Volt. The ramp time is set by the selector switch marked Sweep Time. The sweep time may be set from 1 to 1000 seconds. Two toggle switches control when the ramp is started. When the Start/Reset toggle is at Reset, the Sweep voltage is zero. When the toggle is moved to Start the ramp is started. The Single/Continuous toggle determines what happens when the ramp finishes. When set to Continuous the sweep voltage will be reset to zero and then the ramp will repeat itself. If the Single/Continuous toggle is set to Single, then at the end of the ramp the sweep voltage will remain at the voltage maximum voltage set by the Range potentiometer. This is useful in setting up a sweep. With the toggle at reset (or the Range pot turned to zero) use the Start Field potentiometer to set the starting point for the

⁵ This is with maximum voltage and the current set near the mid point. The pass element will have to dissipate the maximum power, for a given supply voltage, when the pass element voltage is equal to the load voltage, which will be equal to one half of the supply voltage.

sweep. Sweep quickly through the signal, and then use the Range potentiometer to set the end of the sweep.

Ext. Start: It is also possible to control the starting of sweeps electronically. The BNC labeled Ext. Start on the lower front panel accepts TTL signals. With the Start/Reset toggle set to Start, a positive TTL pulse (+5V) on the Ext. Start BNC will reset the sweep voltage to zero. On the falling edge of this pulse the sweep voltage will start to ramp. If the Controller is set to Continuous, the ramp will reset at the end of the ramp and start again. If set to Single, the ramp will stop after one sweep, and remain at the maximum voltage until the next pulse is received.

Modulation Voltage: As has been stated previously, the Reference voltage for the Horizontal Sweep Field is the sum of three different voltages; the Start Field voltage, the Sweep voltage, and the Modulation voltage. The Modulation voltage is derived from the controls labeled Magnetic Filed Modulation on the upper front panel. The circuit for these controls is shown in figure 3E-2.

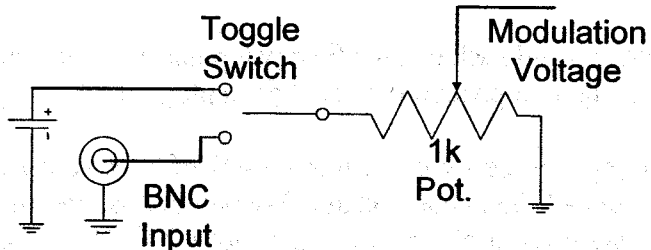


Figure 3E-2 Modulation Voltage Schematic.

They consist of a BNC input, a Start Field /MOD. toggle switch and a one turn potentiometer labeled Amplitude. The Modulation Voltage has several uses. With the toggle switch set to Start Field the BNC input is excluded from the circuit and a small DC voltage is supplied to one side of the potentiometer. The Modulation voltage (which is the voltage on the potentiometer wiper) is then some fraction of this DC voltage. The Modulation voltage thus acts as a fine control of the start field. This is useful when you want to sit right on one of the dips in the Rubidium spectrum. The field range is 0 – 6 mG ($60\mu\text{T}$).

With the Start Field/MOD. toggle in the MOD. position the voltage present on the BNC input is supplied to the potentiometer and becomes the basis for the modulation voltage with the following specifications,

Input Impedance $1\text{k }\Omega$

Maximum Voltage $\pm 20\text{V}$

Voltage - Field conversion $1\text{V} \approx 10\text{mG}$

The modulation input can be used for at least two separate experiments. Magnetic field modulation experiments used in conjunction with Lock-in or AC detection methods.

Secondly large Square wave signals can be applied and the input used for Field Reversal Experiments. (See Experiment section)

Recorder Output and Recorder Offset. The Recorder output is a signal derived from the 1Ω sense resistor that is suitable for driving a chart recorder or oscilloscope. The voltage across the 1Ω sense resistor has been amplified and passed through a low pass filter (time constant = 2 ms.). The signal can also be given a DC offset with ten turn Recorder Offset potentiometer which adds a negative DC voltage to the signal, (-15 Volts at full scale). The gain of the Recorder Output has been set so that $50\text{mV} \approx 1\text{mG}$ (10\mu T), and the voltage can go from -13.5V to +13.5V. When setting up the largest possible sweeps of the instrument the student needs to keep the output within this range.

3F. Radio Frequency

The RF section consists of the following RF coils, 50 Ω current sense resistor and RF amplifier. (See figure 3F-1)

The RF coils are located on the outside of the cell heater.

| | |
|-----------------------------------|------------------------------------|
| Coils | 3 turns/side, 18 gauge copper wire |
| Diameter | 6.45 cm (2.54") |
| Separation | 10.80 cm (4.25") (not Helmholtz) |
| Inductance ⁶ | 1.66 μ H |
| Parallel Capacitance ⁷ | 24 pF |

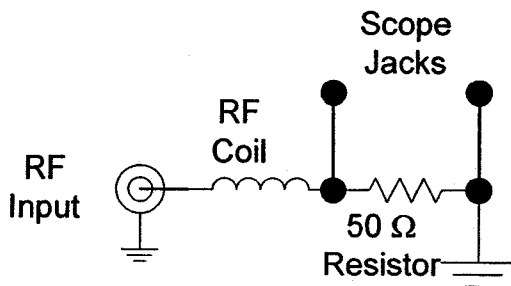


Figure 3F-1 RF Coil and 50 Ω Current Sensing Resistor.

The 50 Ω 0.5 Watt Current Sense Resistor is located in the electrical breakout box on the side of the cell. Oscilloscope probe jacks are on the side of the box so that you may measure the voltage across the resistor and thus measure the current in the coil. We have found that most scope probes are magnetic and would advise you to remove the probe after measuring the current. Because of the nuisance of attaching the probe to the sense resistor the student may be tempted to simply measure the voltage at the output of the amplifier. Thought this would be fine to measure relative changes in RF amplitude at one frequency it will not give an accurate measure of the current at high frequencies due to the effects of the long cable and finite coil impedance.

Radio Frequency Amplifier:

| | |
|------------------------|------------------------------------|
| Input Impedance | 50 Ω |
| Output Impedance | 15 Ω |
| Frequency Range | 10kHz. - 30 MHz. |
| Voltage Gain | 6 V/V |
| Maximum Output Current | 100mA |
| Maximum Output Voltage | 8 V _{p-p} |
| Maximum Output Power | 100 mW |
| Modulation Input | TTL input, 0V = RF on, 5V = RF off |

⁶ Determined from frequency where voltage across coil is equal to voltage across 50 Ω series resistor.

⁷ The capacitance value was not measured directly but is inferred from the resonance at 25 MHz. with $\omega = 1/(L \cdot C)^{1/2}$.

RF AMPLIFIER

Besides the input and output connections on the lower front panel the RF amplifier has a single turn Gain control to adjust the output amplitude. And a TTL RF Modulation Input by which the RF can be modulated on and off. The modulation input can be used with a Lock-in Amplifier or other AC detection technique. The output of the amplifier should be monitor with a oscilloscope to insure that the amplifier is not being overdriven (clipped). A clipped RF output will lead to harmonics and spurious signals.

RF AMPLIFIER

Output of the modulator is:

RF Output of the modulator

The RF output of the modulator is a square wave signal. This signal is generated by a 100 MHz crystal oscillator. The frequency of the oscillator is controlled by a 100 MHz crystal oscillator. The frequency of the oscillator is controlled by a 100 MHz crystal oscillator.

The RF output of the modulator is a square wave signal. This signal is generated by a 100 MHz crystal oscillator. The frequency of the oscillator is controlled by a 100 MHz crystal oscillator.



RF MODULATOR

The RF output of the modulator is a square wave signal. This signal is generated by a 100 MHz crystal oscillator. The frequency of the oscillator is controlled by a 100 MHz crystal oscillator.